

# Pavement Infrastructures Footprint: The Impact of Pavement Properties on Vehicle Fuel Consumption.

A. Louhghalam & M. Akbarian & F.-J. Ulm  
*Massachusetts Institute of Technology  
Cambridge, Massachusetts, United States*

**ABSTRACT:** A novel mechanistic model based on an infinite beam on elastic foundation is developed to quantify the impact of pavement structural and material properties on pavement deflection and consequently on vehicle fuel consumption. The model can also account for the effect of temperature and vehicle speed on fuel consumption. A simplified expression for evaluating the energy dissipation for practical purposes is proposed and used to investigate the impact of various pavement design systems on fuel consumption. GPS (General Pavement Studies) sections from the FHWA's Long Term Pavement Performance program (FHWA 2011) are used for this study. These sections consist of asphalt concrete (AC), portland cement concrete (PCC) and composite pavements. The model quantifies the impact of temperature and vehicle speed on the fuel consumption and confirms that those impacts are negligible for PCC and significant for AC pavements due to their viscoelasticity.

## 1 INTRODUCTION

Road transportation accounts for 27% of all greenhouse gas (GHG) emissions in the United States (EPA 2012). Hence there is growing interest in development of rigorous mechanistic models for assessing pavement sustainability performance in order to reduce carbon footprint of the roadway network. One way to achieve this, is to use Pavement-Vehicle Interaction (PVI) to determine the major contributors to rolling resistance and quantify their impact on the environmental footprint of the transportation system. Pavement texture, roughness and deflection are the relevant factors contributing to the rolling resistance. The dissipated energy and thus fuel consumption due to the deflection-induced pavement-vehicle interaction (PVI) depends on the pavement material and structural properties whereas roughness-induced PVI depends primarily on vehicle characteristics (Zaabar & Chatti 2010). Hence the excess fuel consumption due to pavement deflection, which is related to pavement properties, is studied herein.

Various empirical investigations have examined the dependence of pavement type on deflection-induced PVI (Zaniewski et al. (1982) De Graff (1999), Taylor et al. (2000), Taylor (2002), Taylor and Patten (2006), Ardekani and Sumitsawan (2010) and VEROAD (2002)). The results of these empirical studies, summarized in Figure 1, suggest the dependence of deflection-induced vehicle fuel consumption

on pavement type, but they fail to establish a link between structural and material properties of the pavement and vehicle fuel consumption due to pavement deflection and there is high uncertainty and variability within the suggested values. Another restriction of the empirical approach is the measurement precision required for determining the relatively small change in fuel consumption. While the cumulative fuel consumption difference between pavement types can be large when measured over the pavement's service life, the impact for a single vehicle is quite small. Measurements at this scale, thus will be highly influenced by external factors affecting both the vehicle and the pavement properties and small changes in testing conditions can affect fuel consumption on the same order as any pavement-type effects. In addition to the above reasons the empirical values are not useful for the life cycle assessment of the pavements where a quantitative model is necessary to relate the pavement condition to the carbon footprint of the pavement system.

In this paper we propose a mechanistic model for deflection-induced PVI that quantifies the impact of pavement material and structure on vehicle fuel consumption. In addition, the model also accounts for the effect of temperature and vehicle speed on fuel consumption by considering pavement viscoelasticity. Although the impact of temperature and vehicle speed is small for PCC pavements, to develop a method that can be used for comparative studies in the roadway network, the model must account for these

effects to represent other types of pavements (e.g, viscoelastic AC pavements).

The outline of the paper is as follows: the underlying theory of the mechanistic model is described in Section 2. In Section 3, the mechanistic model is used to evaluate the fuel consumption throughout the United States roadway network and effect of various pavement design systems from the Long Term Pavement Performance program's General Pavement Studies (GPS) sections (FHWA (2011)) is studied. The designs include two types of asphalt concrete (AC) pavements; two types of composite pavements; and three types of Portland cement concrete (PCC) pavement designs. Finally, Section 4 summarizes the findings of this study.

## 2 THEORETICAL ANALYSIS

Consider a pavement structure subjected to a load which moves with the constant speed  $c$ . To maintain this speed, the energy dissipated due to the viscoelasticity of the beam is compensated by the extra power provided by the vehicle, leading to excess fuel consumption.

### 2.1 Dissipated energy

One way to calculate the dissipated energy, i.e. the amount of energy which is not recoverable and is lost in heat form, is through calculation of viscoelastic stresses and strains in the viscoelastic layer, in a fixed coordinate system  $x$ , as the load (tire) passes the pavement, using computational methods such as finite element analysis (Pouget et al. (2011)), and integration over the entire pavement block. To minimize the effect of boundary conditions the pavement block must be sufficiently large. In another approach used herein, the displacement field is calculated in a coordinate system  $X$  which moves with the tire at a constant speed  $c$ , i.e.  $X = x - ct$  where  $t$  is the time variable. In presence of damping, due to the viscoelasticity of the material, the deflection profile becomes asymmetrical and the maximum deflection moves behind the load. Therefore the wheel is always on an uphill slope, resulting in excess rolling resistance (Flügge 1967). Using the second law of thermodynamics, in (Louhghalam et al. 2013a) the authors proved theoretically that the two approaches described above are strictly equivalent and the only difference between the two is the reference frame. The first approach uses a fixed coordinate system attached to the pavement while the latter considers a moving reference frame attached to the tire-pavement contact surface.

Let the pavement structure be an infinite viscoelastic beam on an elastic foundation subjected to a distributed load  $\underline{T} = -pe_z$  moving at a constant speed  $c$  in  $x$ -direction (see Figure 2). The dissipation rate  $\mathcal{D}$  can be evaluated from the second law of thermo-

dynamics (see for example Coussy 1995 and Ulm & Coussy 2002):

$$\mathcal{D} = \delta W - \frac{d\Psi}{dt} \geq 0 \quad (1)$$

with:

$$\delta W = \int_S \underline{T} \cdot \frac{d\underline{u}}{dt} dS \quad (2)$$

the external power supplied to the system,  $\Psi$  the (Helmholtz) free energy and  $\underline{u} = -we_z$  the beam deflection. The total (Lagrangian) derivative  $d/dt$  in the above for any function  $f$  of time and space subjected to velocity field  $\underline{V}$  reads as:

$$\frac{df}{dt} = \frac{\partial f}{\partial t} + \underline{V} \cdot \nabla f \quad (3)$$

with  $\nabla$  representing the gradient vector. In the above moving coordinate system and under steady-state condition (where  $\partial f/\partial t = 0$ ) one can show that the change in free energy is zero (Louhghalam et al. 2013a) and the dissipation rate for an infinite beam on elastic foundation can be obtained as:

$$\mathcal{D} = \delta W = -c \int_S p \frac{\partial w}{\partial X} dS \geq 0 \quad (4)$$

If the traction on the beam is approximately substituted by the resultant concentrated load  $P = \int_S p dS$  the dissipation rate can be simplified as  $\mathcal{D} = -cbP dw/dX$  with  $b$  the width of the beam. For the elastic case where there is no dissipation, the slope is zero at pavement-tire contact point, confirming that the maximum displacement occurs exactly below the tire. Furthermore the non-negativity of the dissipation rate requires that  $dw/dX \leq 0$  which indicates that the tire is on an upward slope as shown in Figure 2 (b) (Flügge 1967).

The above analysis indicates that for evaluating the dissipated energy one only needs to find the displacement profile at the tire-pavement contact surface in the moving coordinate system.

### 2.2 Viscoelastic beam on elastic foundation

Let  $h$  be the thickness of the infinite viscoelastic beam and  $k$  be the Winkler modulus of the elastic foundation. The viscoelasticity of the beam is modeled using the Maxwell model with stiffness  $E$  and viscosity  $\eta$  (see the inset of Figure 2(a)) for which the constitutive equation is  $\sigma + \tau\dot{\sigma} = \tau E\dot{\epsilon}$ , where  $\tau = \eta E$  is the relaxation time of the viscoelastic material that varies with temperature, leading to temperature dependent mechanical properties for viscoelastic material. The time-temperature superposition principle is used to establish this temperature dependence and to find the relaxation time of the material at any given temperature  $T$  from the relaxation time measured at a reference temperature  $T_{ref}$ :

$$\tau(T) = a_T \times \tau(T_{ref}) \quad (5)$$

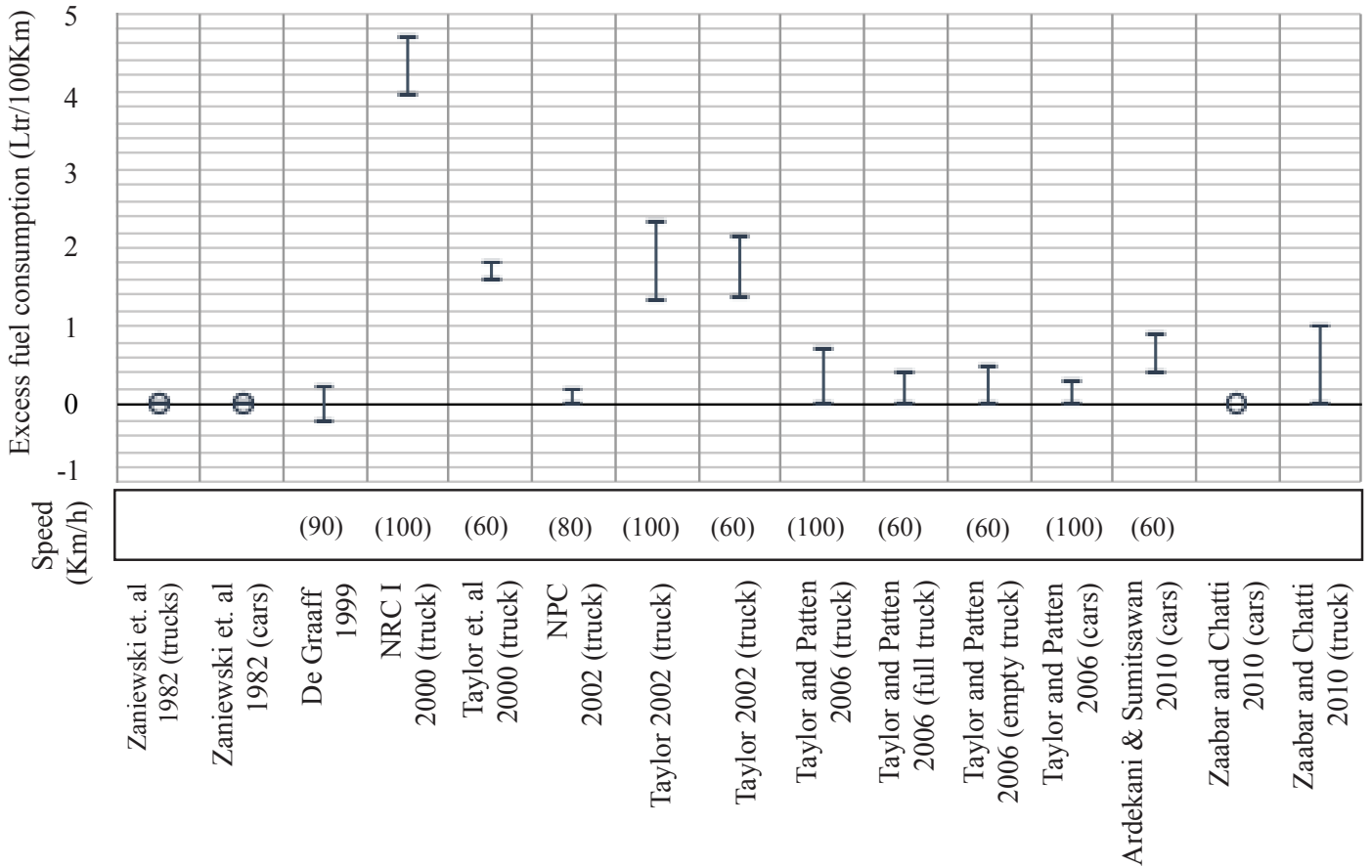


Figure 1: Empirical evaluation of fuel consumption; the values are presented as increase in fuel consumption of AC pavements relative to concrete pavement, "o" represent zeros and the negative value indicates that the fuel consumption of concrete is greater than asphalt pavement

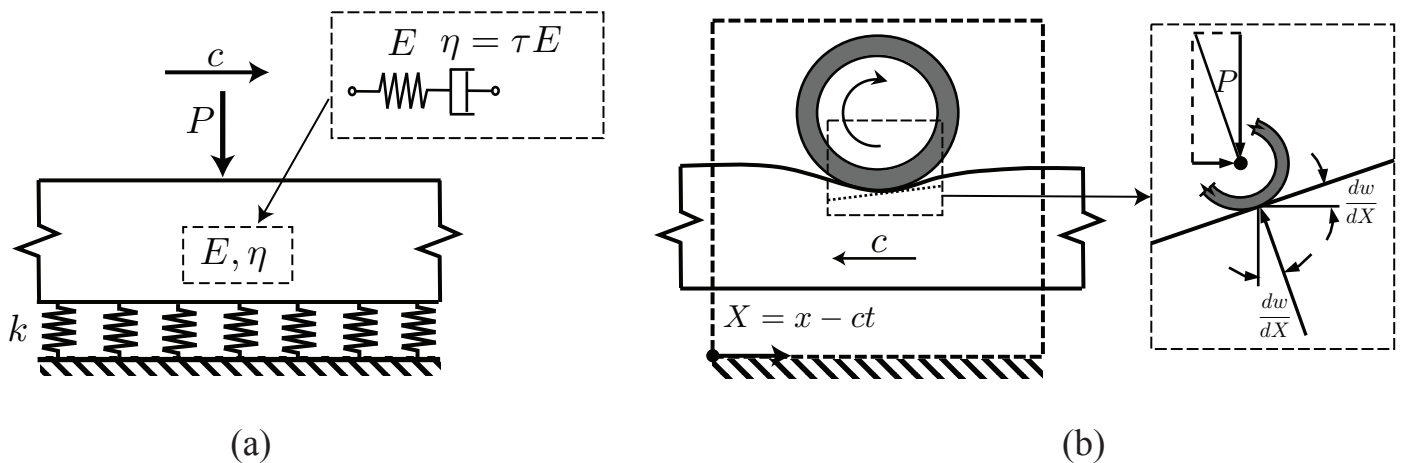


Figure 2: (a): Infinite viscoelastic beam on elastic foundation; Maxwell viscoelastic model is illustrated in inset; (b): Wheel is on an uphill slope in the moving coordinate system, with magnified slope in inset

where  $a_T$  is the shift factor calculated from the Arrhenius law:

$$\log a_T(T) = U_c \left[ \frac{1}{T} - \frac{1}{T_{ref}} \right] \quad (6)$$

for concrete pavements (Bazant 1995) and from William Ferry Landel equation:

$$\log a_T(T) = \frac{-c_1(T - T_{ref})}{c_2 + (T - T_{ref})} \quad (7)$$

for asphalt pavements (Pouget et al. 2011).

To determine the displacement profile of a viscoelastic beam on elastic foundation, the elastic-viscoelastic correspondence principle is used (see Read (1950), Pozhuev (1986), Christensen (1982) among many other sources). The elastic solution is obtained from the equation of motion for an infinite elastic beam on elastic foundation in the moving coordinate system where  $d/dt = -cd/dX$ :

$$\frac{Eh^3}{12} \frac{\partial^4 w}{\partial X^4} + mc^2 \frac{\partial^2 w}{\partial X^2} + kw = p \quad (8)$$

with  $m$  mass per unit area of the beam. Taking the Fourier transform of the above equation the Fourier transform of elastic response can be determined:

$$\hat{w} = \frac{\hat{p}}{Eh^3\lambda^4/12 - mc^2\lambda^2 + k} \quad (9)$$

where  $\lambda$  is the transformed field of  $X$  and  $\hat{\cdot}$  represents the Fourier transform. The constitutive equation for Maxwell model in the moving coordinate system:

$$\sigma - c\tau \frac{d\sigma}{dX} = -c\tau E \frac{d\epsilon}{dX} \quad (10)$$

is then used to obtain its complex modulus:

$$E^* = -\frac{i\lambda c\tau}{1 - i\lambda c\tau} E \quad (11)$$

which is subsequently substituted for  $E$  in equation (9):

$$\hat{w} = \frac{\hat{p}}{-i\lambda^5 c\tau E h^3/12(1 - i\lambda c\tau) - mc^2\lambda^2 + k} \quad (12)$$

Based on the elastic-viscoelastic correspondence principle (Pozhuev 1986) the inverse Fourier transformation of the above equation yields the displacement profile for an infinite Maxwell viscoelastic beam on elastic foundation. The slope profile of the beam is determined by taking the inverse Fourier transform of  $i\lambda\hat{w}$ , implemented numerically herein using the Fast Fourier Transform algorithm (Cooley & Tukey 1965). Finally the dissipation rate is evaluated from equation (4).

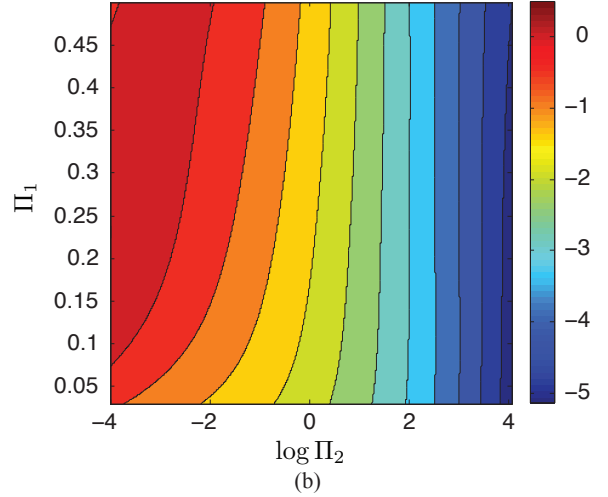
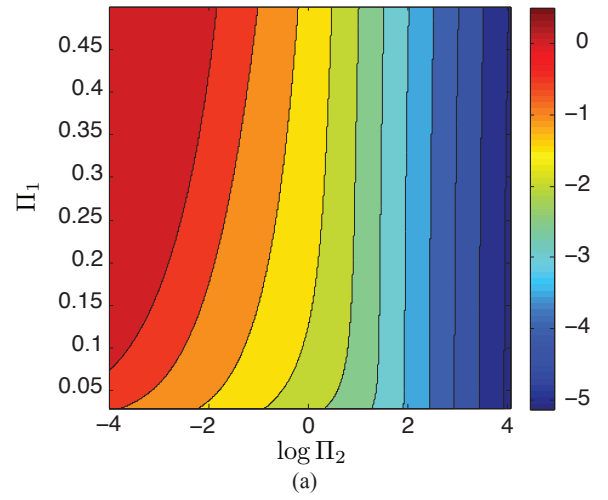


Figure 3: Contour plot of logarithm of dimensionless dissipation  $\log_{10} \Pi = \log_{10} \mathcal{D}bc_{cr}/P^2$  versus the two invariants  $\Pi_1$  and  $\Pi_2$  (a): with  $\mathcal{D}$  evaluated from (4) (b): with  $\Pi$  evaluated from the simplified fit in (14)

### 2.3 Simplified dissipation model for practical purposes

Evaluation of dissipated energy by numerically solving the equation of motion is complex for practical purposes such as engineering applications and network life cycle analyses. To overcome this issue and to obtain a simple method for evaluating the dissipated energy, we use the result of dimensional analysis (Louhghalam et al. 2013b) along with the numerical method explained in Sections 2.1 and 2.2 to determine the functional relationship between the dimensionless dissipation rate  $\Pi = \mathcal{D}bc_{cr}/P^2$  and the invariants of the problem:

$$\Pi_1 = \frac{c}{c_{cr}} \quad \Pi_2 = \tau \sqrt{\frac{k}{m}} \quad (13)$$

where  $c_{cr} = \sqrt[4]{Eh^3k/12m^2}$ . Figure 3(a) shows the variation of dimensionless dissipation rate  $\Pi$  versus  $\Pi_1$  and  $\Pi_2$ . Linear regression is then used to fit a two dimensional surface to the function shown in Figure 3(a) for  $0.03 \leq \Pi_1 \leq 0.5$  and  $0.0001 \leq \Pi_2 \leq 12,000$ :

$$\log_{10} \Pi = \sum_{i=0}^5 \sum_{j=0}^3 p_{ij} \Pi_1^i \times (\log_{10} \Pi_2)^j \quad (14)$$

Table 1: Coefficients  $p_{ij}$  with 95% confidence intervals.

| j \ i | 0                                   | 1                          | 2                             | 3                          | 4                          | 5                       |
|-------|-------------------------------------|----------------------------|-------------------------------|----------------------------|----------------------------|-------------------------|
| 0     | -1.918<br>(-1.922, -1.915)          | 4.487<br>(4.379, 4.596)    | -19.54<br>(-20.64, -18.44)    | 59.58<br>(54.61, 64.55)    | -92.51<br>(-102.6, -82.39) | 56.23<br>(48.63, 63.83) |
| 1     | -0.4123<br>(-0.4135, -0.4111)       | -1.802<br>(-1.824, -1.78)  | 4.014<br>(3.864, 4.163)       | -4.628<br>(-5.04, -4.217)  | 1.375<br>(0.9895, 1.761)   | -                       |
| 2     | -0.06942<br>(-0.06969, -0.06915)    | 0.2153<br>(0.2111, 0.2194) | -0.8618<br>(-0.8794, -0.8441) | 0.7344<br>(0.7124, 0.7563) | -                          | -                       |
| 3     | -0.009575<br>(-0.009656, -0.009495) | 0.0203<br>(0.0196, 0.021)  | 0.04669<br>(0.04542, 0.04797) | -                          | -                          | -                       |

Table 2: General Pavement Studies (GPS) sections from the LTPP program (FHWA 2011)

| GPS Number | Description   | Pavement Type |
|------------|---|---------------|
| GPS-1      | Asphalt Concrete Pavement on Granular Base            | AC            |
| GPS-2      | Asphalt Concrete Pavement on Stabilized Base          |               |
| GPS-3      | Jointed Plane Concrete Pavement                       | PCC           |
| GPS-4      | Jointed Reinforced Concrete Pavement                  |               |
| GPS-5      | Continuously Reinforced Concrete Pavement             |               |
| GPS-6      | Asphalt Concrete Overlay of Asphalt Concrete Pavement | Composite     |
| GPS-7      | Asphalt Concrete Overlay of PCC Pavement              |               |

with regression coefficients  $p_{ij}$  given in Table 1. The dimensionless dissipation rate evaluated from the fitted function in (14) is illustrated in Figure 3(b) for comparison.

The calibration and validation of model is discussed in detail in Louhghalam et al. (2013b) and performed by estimating the relaxation time  $\tau(T_{ref}) = 0.0083$  at the reference temperature  $T_{ref} = 10$  that fits closely to the data in literature.

### 3 NETWORK ANALYSIS

The impact of deflection-induced PVI on the fuel consumption within the United State roadway network is investigated in this section. The simplified mechanistic model developed in Section 2.3 is applied to the data from FHWA's Long-Term Pavement Performance (LTPP) program (FHWA 2011) to examine the impact of pavement design on pavement deflection and thus the excess fuel consumption.

#### 3.1 Data description

The data used herein, consist of more than 800 pavement sections from the General Pavement Studies (GPS) program of the LTPP database, from in-service test sections in either the original design phase or after the first overlay. The sections include asphalt concrete (AC), portland cement concrete (PCC) and composite pavement designs as described in Table 2. Under the

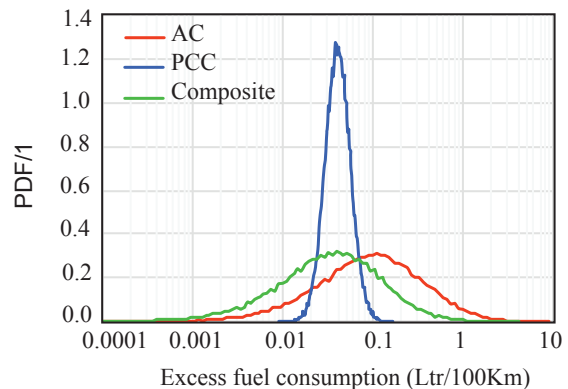


Figure 4: Probability distribution of excess fuel consumption for each pavement type evaluated for an HS20-44 truck traveling at a constant speed of  $c=100$  Km/h and at a moderate temperature  $10^{\circ}\text{C} \pm 10^{\circ}\text{C}$ .

LTPP's GPS program, climatic data, material properties, traffic frequency, deflection profile, distress, and friction data were collected for each section. The GPS sections represent material and structural pavement designs used in engineering practices throughout the United States.

For each section, the top layer and subgrade moduli  $E$  and  $G_s$  are estimated using the arrival time of the signal from Falling Weight Deflectometer (FWD) time history data along with the wave propagation theory (Akbarian et al. 2012) and compared with the back calculated quantities reported in LTPP database (FHWA 2011). The probability distribution function for pavement modulus  $E$ , subgrade modulus  $G_s$  as well as pavement thickness  $h$  are evaluated for each GPS section (Louhghalam et al. 2013b). These distributions approximately follow lognormal distribution with the mean value and standard deviation of their corresponding normal distribution presented in Table 3.

#### 3.2 Results and discussions

The probability distributions for the GPS sections are used along with the simplified mechanistic PVI model in (14) in a Monte-Carlo simulation setting to evaluate the probability distribution function for the dissipated energy due to deflection-induced PVI in units of energy per traveled length (MJ/Km). The results are then converted to fuel consumption (Ltr/Km) via EPA's MPG equivalent rating of Gasoline, i.e. 32.05

Table 3: Mean-value, standard deviation and coefficient of variation of the corresponding normal distribution for pavement modulus  $E$  (in  $\ln(\text{MPa})$ ), subgrade shear modulus  $G_s$  (in  $\ln(\text{MPa})$ ) and pavement thickness  $h$  (in  $\ln(\text{m})$ ) for GPS-section categories (FHWA 2012)

| GPS No | $\mu_{\ln(E)}$ | $\sigma_{\ln(E)}$ | $\text{COV}_{\ln(E)}$ | $\mu_{\ln(G_s)}$ | $\sigma_{\ln(G_s)}$ | $\text{COV}_{\ln(G_s)}$ | $\mu_{\ln(h)}$ | $\sigma_{\ln(h)}$ | $\text{COV}_{\ln(h)}$ |
|--------|----------------|-------------------|-----------------------|------------------|---------------------|-------------------------|----------------|-------------------|-----------------------|
| GPS-1  | 8.9491         | 0.6632            | 0.0741                | 5.4393           | 0.5285              | 0.0972                  | -1.8524        | 0.5718            | -0.3087               |
| GPS-2  | 9.0151         | 0.6378            | 0.0707                | 5.7375           | 0.4997              | 0.0871                  | -1.7556        | 0.5618            | -0.3200               |
| GPS-3  | 10.4086        | 0.2540            | 0.0244                | 5.3498           | 0.3705              | 0.0693                  | -1.4048        | 0.1079            | -0.0768               |
| GPS-4  | 10.4603        | 0.1588            | 0.0152                | 5.4723           | 0.2636              | 0.0482                  | -1.3684        | 0.0515            | -0.0376               |
| GPS-5  | 10.3903        | 0.2485            | 0.0239                | 5.5017           | 0.3805              | 0.0692                  | -1.5135        | 0.0892            | -0.0589               |
| GPS-6  | 9.0928         | 0.9506            | 0.1045                | 6.0642           | 0.6308              | 0.1040                  | -1.4827        | 0.5278            | -0.3560               |
| GPS-7  | 9.1184         | 0.8796            | 0.0965                | 6.7312           | 0.7609              | 0.1130                  | -1.4297        | 0.2233            | -0.1562               |

MJ/Ltr. The GPS sections are combined into three major pavement types (AC, PCC and composite pavements) as shown in Table 2. For an HS20-44 truck with axle loads  $P_1 = 36.29$  kN,  $P_2 = P_3 = 145.15$  kN, traveling at a constant speed  $c = 100$  km/h and at temperature  $10^\circ\text{C} \pm 10^\circ\text{C}$  the distribution of excess fuel consumption due to deflection-induced PVI is illustrated in Figure 4. The peaks of probability distribution for composite and PCC pavement occur at almost equal fuel consumption although the PCC pavement has a narrower distribution. This is due to narrower probability distribution functions for both pavement stiffness and thickness (see the corresponding coefficients of variation in Table 3). The excess fuel consumption in AC pavements is higher compared to PCC and composite pavement material and its probability distribution is wider due to wider distribution of pavement thickness in the network.

The impact of temperature and speed on the extra fuel consumption is also studied for the three pavement material types. Figure 5(a) and (b) illustrate the extra fuel consumption at the 95% confidence level for the HS20-44 truck as a function of speed and at temperatures  $10^\circ\text{C} \pm 10^\circ\text{C}$  and  $30^\circ\text{C} \pm 10^\circ\text{C}$  respectively. The fuel consumption due to deflection-induced PVI decreases significantly for AC pavements with speed. The changes of fuel consumption due to speed are more significant at higher temperatures. The variation of fuel consumption as a function of temperature for a constant speed  $c = 100$  Km/h is presented in Figure 5(c). The results confirm the significant change in fuel consumption in asphalt concrete pavements as a result of temperature variations. The excess fuel consumption in PCC pavements does not change significantly with speed and temperature as expected and the moderate variation in composite pavements is due to the temperature and speed dependent mechanical properties of the viscoelastic layer.

The sustainability performance of AC and PCC pavements at different climatic conditions are investigated throughout the United States. The excess fuel consumption of an HS20-44 truck traveling at  $c = 100$  Km/h at annual mean temperatures (NOAA 2013) of different states is illustrated in Figure 6(a) and (b) for asphalt and concrete pavements respectively. While for PCC sections, the excess fuel consumption due to

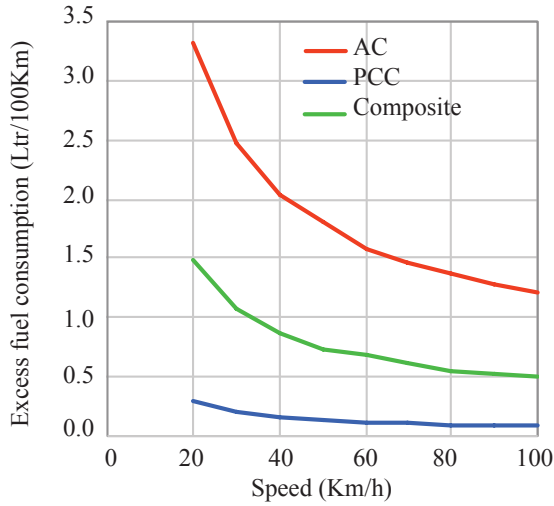
pavement deflection at 95 % confidence level varies slightly from 0.0719 to 0.0952 Ltr/100Km, for the AC pavements the fuel consumption changes significantly from 0.2073 Ltr/100Km in North Dakota to 1.4647 Ltr/100Km in Florida. It is worth noting that the excess fuel consumption evaluated herein is only due to the deflection of the pavement and the impact of pavement roughness which is also temperature dependent is not taken into account.

#### 4 CONCLUSIONS

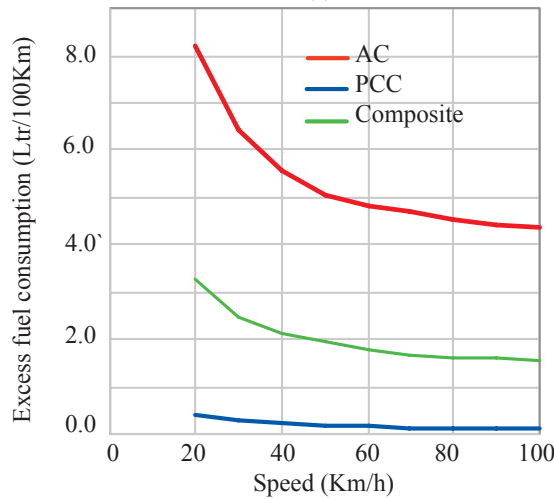
To establish a framework for the design of sustainable transportation system, it is necessary to assess the environmental footprint of the pavements. The mechanistic model developed herein provides a rigorous tool for quantifying the impact of different material and structural properties on the pavement deflection and the associated fuel consumption. The model is based on an infinite viscoelastic beam on elastic foundation. The results of theoretical analysis presented in Figure (3) shows that for a specified value of  $\Pi_2$  the variation of dimensionless dissipation rate with respect to the dimensionless speed is insignificant. Therefore the dissipation rate is approximately proportional to the axle load  $P^2$  and inversely proportional to  $E^{1/4}$ ,  $h^{3/4}$  and  $k^{1/4}$  and doubling the thickness of the pavement, as an example, leads to 40% decrease in the dissipated energy and thus fuel consumption.

Moreover the viscoelasticity of the pavement layer allows for accounting for the impact of temperature and speed. The non-dimensional dissipation and therefore the fuel consumption is related inversely to  $\Pi_2$  and thus directly to temperature. This is also observed in the road network analysis results shown in Figures 5(c) and 6. The fuel consumption per unit length of the pavement due to deflection-induced PVI is also inversely related to speed. The dependency to temperature and speed, however, is shown to be insignificant for the PCC pavements where the viscoelasticity of the pavement material is negligible.

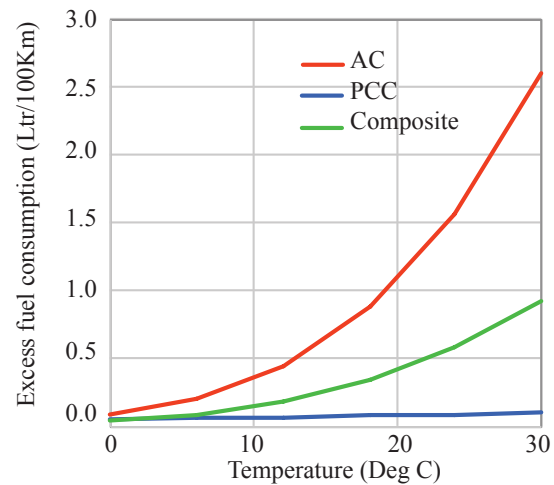
The above results suggest that for given environmental conditions (e.g. temperature) and road types (vehicle speed) the dissipated energy can be used as a criterion in choosing pavement structural and material properties to achieve a sustainable pavement design.



(a)

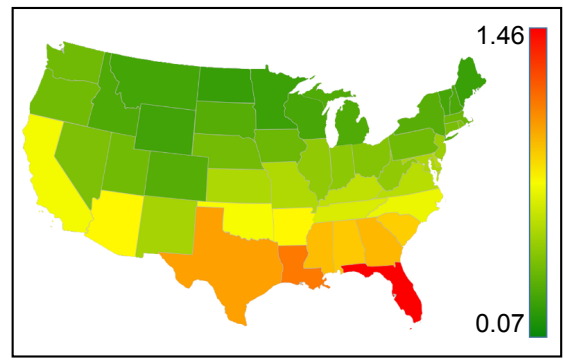


(b)

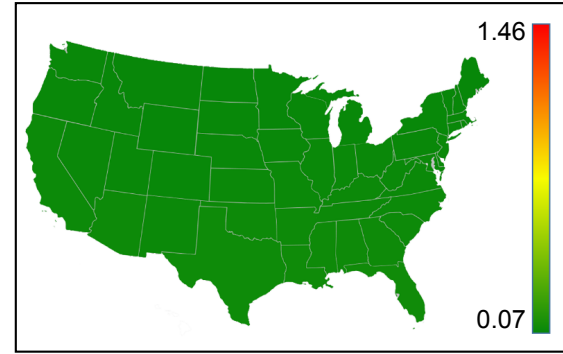


(c)

Figure 5: Variation of excess fuel consumption at the 95% confidence level as a function of (a): speed at  $T=10^{\circ}\text{C}\pm 10^{\circ}\text{C}$ ; (b): speed at  $T=30^{\circ}\text{C}\pm 10^{\circ}\text{C}$  (c): temperature at  $c=100\text{ Km/h}$



(a)



(b)

Figure 6: Excess fuel consumption (Ltr/100Km) of an HS20-44 truck evaluated at annual mean temperatures across the United States for (a): AC sections; (b): PCC sections

## 5 ACKNOWLEDGMENT

This research was carried out by the CSHub@MIT with sponsorship provided by the Portland Cement Association (PCA) and the Ready Mixed Concrete (RMC) Research & Education Foundation. The CSHub@MIT is solely responsible for content.

## REFERENCES

- Akbarian, M., S. S. Moeini-Ardakani, F.-J. Ulm, & M. Nazzal (2012). Mechanistic approach to pavement-vehicle interaction and its impact on life-cycle assessment. *Transportation Research Record: Journal of the Transportation Research Board* 2306(1), 171–179.
- Ardekani, S. A. & P. Sumitsawan (2010). Effect of pavement type on fuel consumption and emissions in city driving.
- Bazant, Z. (1995). Creep and damage in concrete. *Materials science of concrete IV*, 355–389.
- Christensen, R. (1982). *Theory of viscoelasticity: an introduction*. Academic press.
- Cooley, J. W. & J. W. Tukey (1965). An algorithm for the machine calculation of complex fourier series. *Mathematics of computation* 19(90), 297–301.
- Coussy, O. (1995). *Mechanics of porous continua*. Wiley.
- De Graff, D. (1999). *Rolling resistance of porous asphalt, a pilot study (in Dutch)*.
- EPA (Accessed 2012). 2009 u.s. greenhouse gas inventory report. environmental protection agency.
- FHWA (Accessed 2011). Long-term pavement performance program. 2011[online].
- Flügge, W. (1967). *Viscoelasticity*. Springer Verlag.
- Louhghalam, A., M. Akbarian, & F.-J. Ulm (2013a). Flügge's conjecture: Dissipation vs. deflection induced pavement-vehicle-interactions (pvi). *Journal of Engineering Mechan-*

ics accepted.

- Louhghalam, A., M. Akbarian, & F.-J. Ulm (2013b). Scaling relations of dissipation-induced pavement-vehicle interactions. *Transportation Research Record: Journal of the Transportation Research Board* under review.
- NOAA (2013). National oceanic and atmospheric administration [online] accessed 2013.
- Pouget, S., C. Sauzéat, H. D. Benedetto, & F. Olard (2011). Viscous energy dissipation in asphalt pavement structures and implication for vehicle fuel consumption. *Journal of Materials in Civil Engineering* 24(5), 568–576.
- Pozhuev, V. (1986). Steady-state reaction to the effect of a moving load in a system consisting of a cylindrical shell and a viscoelastic filler. *International Applied Mechanics* 22(5), 415–421.
- Read, W. T. (1950). Stress analysis for compressible viscoelastic materials. *Journal of Applied Physics* 21(7), 671–674.
- Taylor, G. (2002). Additional analysis of the effect of pavement structure on truck fuel consumption. *Ottawa: Cement Association of Canada*.
- Taylor, G., P. Marsh, & E. Oxelgren (2000). Effect of pavement surface type on fuel consumption-phase ii: Seasonal tests. *Portland Cement Association, CSTT-HWV-CTR-041, Skokie, IL*.
- Taylor, G. & J. Patten (2006). Effects of pavement structure on vehicle fuel consumption-phase iii.
- Ulm, F.-J. & O. Coussy (2002). *Mechanics and durability of solids: Solid Mechanics, Vol 1*. Prentice Hall.
- VEROAD (2002). Maximum energy dissipation when driving on asphalt pavement versus driving on rigid cement concrete. *Netherlands Pavement Consultants*.
- Zaabar, I. & K. Chatti (2010). Calibration of hdm-4 models for estimating the effect of pavement roughness on fuel consumption for us conditions. *Transportation Research Record: Journal of the Transportation Research Board* 2155(1), 105–116.
- Zaniewski, J. P., B. Butler, G. Cunningham, G. Elkins, & M. Paggi (1982). Vehicle operating costs, fuel consumption, and pavement type and condition factors. Technical report.